

Connection of microstructure to rheology in a microemulsion model

Gerald Pätzold* and Kenneth Dawson

*Advanced Computational Research Group, Centre for Soft Condensed Matter and Biomaterials, Department of Chemistry,
University College Dublin, Belfield, Dublin 4, Ireland*

(Received 19 January 1996)

The rheological properties of self-assembling fluids are studied within the framework of a simple time-dependent Landau-Ginzburg model. In addition to the Langevin relaxation dynamics, the order parameter field is subject to a kinematic deformation process due to a shear velocity field. The Hamiltonian contains a Gaussian part which has proven to be important in the study of self-assembly, as well as ϕ^4 and $\phi^2(\nabla\phi)^2$ contributions. In the disordered phase and for low shear rate, the relevant rheological coefficients (excess viscosity, first and second normal stress coefficient) can be calculated perturbatively. The essential ingredient is the one-loop, self-consistent solution of the evolution equation for the quasistatic structure factor. In the case of steady shear, we find shear thinning behavior, a positive first, and a negative second normal stress difference for all values of the shear rate. For oscillatory shear, it turns out that the self-assembling structures give rise to viscoelastic behavior. Analytic results are derived for the limiting cases of low and high frequency. For low steady shear, all results can be expressed in scaling form using the correlation lengths d and ξ originally defined for microemulsion under equilibrium conditions and scaling functions already known from the pure Gaussian treatment. This suggests a class of experiments where neutron scattering data can be compared to viscosity results. For low to high shear rates, the one-loop equations have also been solved numerically, and we display the nonequilibrium structure factors arising from this approach. [S1063-651X(96)08708-9]

PACS number(s): 82.70.Kj, 83.70.Hq, 83.50.Ax, 83.20.Jp

INTRODUCTION

As a reasonable understanding of equilibrium self-assembly phenomena has emerged it has become more apparent that many of the most important issues for technological applications have hardly been studied, let alone understood. One of these, the connection between microstructure and rheology, or stress relaxation, is of fundamental importance in diverse areas such as, for example, understanding of consistency in the food industry, the quality of paints, cosmetics, and numerous other products. We wish to contribute some theoretical and numerical results, but emphasize that there remains much uncertainty even about the validity of various models. What follows must be viewed as part of the process of defining the model, and the tools that can be applied in this field.

In self-assembling fluids, correlated mesoscopic structures exist even far from criticality. The deformation of these domains under an imposed flow gives rise to excess stresses. This results in rheological behavior that is quite different to that familiar from simple Newtonian liquids. When the complex fluid approaches criticality, the correlation length describing the linear extension of the mesoscopic structures diverges. Then even weak shear leads to significant structural deformations, since any diffusion process is slow to restore the displacements caused by the kinematics of the flow field. Clearly changes in the rheological properties become even more pronounced on approach to criticality, but for self-

assembled phases it is already of interest to understand the problem somewhat away from the critical point. Much of what we describe below finds its roots in a lattice model due to Widom [1] whose subsequent success in equilibrium rationalizations provides the basis for much modern work.

In a previous paper [2], we have investigated the rheology of self-assembled fluids based on a Gaussian model both theoretically and, in particular, by direct Langevin simulation of a two-dimensional microemulsion with nonconserved order parameter under shear. We now turn to three space dimensions with conserved order parameter and have also included non-Gaussian terms to account for the effect of large fluctuations and to study the consequences of mode coupling. The direct Langevin simulations are a much greater computation challenge in three dimensions, so we restrict ourselves to the level of a self-consistent closed evolution equation for the quasistatic structure factor. Otherwise the extensive parameter studies to check scaling behavior and the treatment of oscillatory shear would not have been possible.

The behavior of self-assembled phases in nonequilibrium conditions was first addressed in Ref. [3] on rheology and [4] on kinetics, but the discussion is now being broadened by others [5–7]. Related rheological investigations have been carried out for critical binary mixtures [8] and for block copolymer melts, first in the mean field approximation [9,10], and later on including mode coupling and fluctuation effects both in the order parameter and the velocity field [11]. Questions similar to the ones considered by us also arise in the investigation of the effects of shear flow on the turbidity of critical colloidal dispersions [12].

The outline of the paper is as follows. In the next section, we introduce the model in terms of a Hamiltonian for a single scalar order parameter and a system of time-dependent Landau-Ginzburg equations for order parameter and velocity

*Present address: Institut für Theoretische Physik, Universität Heidelberg, Philosophenweg 19, D-69120 Heidelberg, Germany. Electronic address: paetzold@tphys.uni-heidelberg.de; WWW address: <http://wwwcp.tphys.uni-heidelberg.de/~paetzold/>

field. The velocity field is then fixed in order to subject the fluid to the simplest viscometric flow. We state the functionals which relate the rheological coefficients—excess viscosity, first and second normal stress coefficient—to the quasistatic structure factor. The section closes with the full nonlinear stochastic evolution equation for the order parameter under shear flow and the equation for the quasistatic structure factor derived self-consistently in the one-loop approximation.

The next section is concerned with the case of steady shear. For completeness, we first turn to the Gaussian case and derive an integral representation for the steady-state structure factor under shear flow. As a preliminary step, we then compute the self-consistent, loop-corrected structure factor with the shear set to zero. The result can be freed from the microscopic parameters in favor of the experimentally accessible correlation lengths. We then pursue the perturbative calculation of the structure factor for small values of the shear rate and in the presence of loop corrections. We calculate up to second order in the shear rate and derive scaling forms for excess viscosity and the normal stress coefficients. The scaling relations are checked by numerical work, which becomes essential when studying the non-Newtonian behavior, that is the shear-rate dependence of the rheological coefficients, of the model. For comparison to experimental work, we also show grey-scale plots of the structure factor for various shear rates. We finally discuss the asymptotic scaling for very high shear.

The next section is devoted to oscillatory shear. We consider the linear response regime and give formulations of the stress in terms of a complex shear modulus and a complex viscosity. We then solve the loop-corrected evolution equation for the quasistatic structure factor for oscillatory shear up to first order in the shear rate. This allows us to derive integral representations in wave number space for the frequency-dependent real and imaginary parts of the complex viscosity. For arbitrary shear frequency, these integrals have been fully evaluated numerically and viscoelastic behavior is discussed. However, for small frequency, a Taylor expansion with the steady-state result for the viscosity as the zeroth-order term is valid. Also an asymptotic result for very high frequency is presented.

Numerical methods have been useful to check analytical results and to make progress where an explicit solution could not be found. We therefore include a short section to discuss some schemes to solve the self-consistent evolution equation for the quasistatic structure factor numerically. Finally, in a concluding section, we summarize and discuss the results found and indicate the possibilities for further work.

MODEL

In this paper, we are concerned with the rheological properties of self-assembling fluids as far as they can be derived from a simple Landau-Ginzburg model for a scalar order parameter based on the Hamiltonian

$$H[\phi] = \int d^Dx \left[\frac{c}{2} (\vec{\nabla}^2 \phi)^2 + \frac{1}{2} (g_0 + g_2 \phi^2) (\vec{\nabla} \phi)^2 + \frac{a_2}{2} \phi^2 + \frac{\lambda}{4!} \phi^4 \right]. \quad (1)$$

The Gaussian part of this functional has proven to be the essential ingredient when modeling the basic features of self-assembling fluids such as microemulsions. It is suggested by the fitting of scattering data [13] and by the analysis of a lattice model due to Widom [1,14]. The higher-order terms have been proposed based upon phenomenological reasoning. Extensive work has been carried out on this and other formulations of the theory [1,14,15] and a consensus has been reached that the equilibrium structure is reasonably well understood. In the following, we are mainly interested in the disordered but structured region of the phase diagram where $a_2 > 0$ and $g_0^2 \lesssim 4a_2c$. The non-Gaussian terms in Eq. (1) allow us to consider two types of phase transitions observed in self-assembling systems. First, if a_2 becomes negative, we enter the three-phase coexistence region and meet spinodal decomposition. In order to have a Hamiltonian that is bounded from below in this region, and furthermore to capture the fluctuation effects in the critical region, the quartic term $(\lambda/4!) \phi^4$ is included. Second, negative values of the bare interfacial tension g_0 favor the formation of interfaces. However, this effect of decreased effective interfacial tension should only be present where the gradient of the order parameter is large, that is in the region where surfactant gathers, but not within the bulk phases. Furthermore, if g_0 is decreased such that $g_0 \lesssim -\sqrt{4a_2c}$, we expect the formation of lamellar phases. We therefore also include the term $(g_2/2) \phi^2 (\nabla \phi)^2$ for completeness, but it is numerically not very significant in much of what follows.

The time-dependent Landau-Ginzburg equations for order parameter and velocity field constitute a stochastic gradient dynamics with mode coupling terms [16],

$$\frac{\partial \phi}{\partial t} + \vec{\nabla} \cdot (\phi \vec{v}) = \Gamma_\phi \frac{\delta \mathcal{H}}{\delta \phi} + \eta_\phi, \quad (2)$$

$$\frac{\partial \vec{v}}{\partial t} + \vec{\nabla} \cdot (\vec{v} \vec{v}) = \eta_0 \vec{\nabla}^2 \vec{v} + \sigma_0 \vec{\nabla} \cdot (\vec{\nabla} \cdot \vec{v}) - \phi \vec{\nabla} \frac{\delta \mathcal{H}}{\delta \phi} + \vec{\eta}_v. \quad (3)$$

In particular, the order parameter field ϕ is convected by the velocity field \vec{v} . We assume that in the absence of fluctuations the fluid can be characterized by a bare shear viscosity η_0 and a bare bulk viscosity σ_0 . However, we only treat the incompressible case $\vec{\nabla} \cdot \vec{v} = 0$ in what follows, and the bulk viscosity is of no further relevance. The coupling between ϕ and \vec{v} in Eq. (2) implies a third term on the right-hand side of Eq. (3) such that $\exp[-H - \int d^Dx (|\vec{v}|^2/2)]$ is the joint equilibrium distribution of ϕ and \vec{v} [10,16]. This coupling term in the velocity equation also gives rise to the excess stress tensor to be considered in the following discussion. We restrict ourselves to the physically most relevant case, that of three space dimensions and conserved order parameter. The kinetic coefficient is then given by $\Gamma_\phi = \Gamma \vec{\nabla}^2$, and the fluctuation-dissipation theorem requires the correlations for the Gaussian noise terms,

$$\langle \eta_\phi(\vec{x}, t) \eta_\phi(\vec{x}', t') \rangle = -2T \Gamma_\phi \delta(\vec{x} - \vec{x}') \delta(t - t'), \quad (4)$$

$$\langle \eta_i(\vec{x}, t) \eta_j(\vec{x}', t') \rangle = -2TL_{ij} \delta(\vec{x} - \vec{x}') \delta(t - t'), \quad (5)$$

where $L_{ij} = \eta_0 \vec{\nabla}^2 \delta_{ij} + \sigma_0 \vec{\nabla}_i \vec{\nabla}_j$, and the ‘‘temperature’’ T is a free parameter that adjusts the noise intensity. We neglect hydrodynamic fluctuations and subject the system to the simplest viscometric shear flow [17],

$$\vec{v} = \dot{\gamma}(t) y \vec{e}_x, \quad (6)$$

where the shear rate, $\dot{\gamma}(t)$, may depend on time.

As shown previously by others in a related context [8–10], and made explicit for self-assembly in our previous papers [2,3], there is, in a system which is spatially homogeneous on average, a close link between the structure factor and the excess stresses of rheological interest. Starting from the coupling in Eq. (3), it can be shown that the stresses are given as integrals of the nonequilibrium structure factor, dressed with characteristic weight factors, over wave number space. To be explicit, we calculate the shear stress, the first, and the second normal stress difference according to

$$\sigma_{xy}(t) = - \int \frac{d\mathbf{k}}{(2\pi)^D} k_x k_y (g_R + 2ck^2) S(\mathbf{k}, t), \quad (7)$$

$$\begin{aligned} N_1(t) &= \sigma_{xx}(t) - \sigma_{yy}(t) \\ &= - \int \frac{d\mathbf{k}}{(2\pi)^D} (k_x^2 - k_y^2) (g_R + 2ck^2) S(\mathbf{k}, t), \end{aligned} \quad (8)$$

$$\begin{aligned} N_2(t) &= \sigma_{yy}(t) - \sigma_{zz}(t) \\ &= - \int \frac{d\mathbf{k}}{(2\pi)^D} (k_y^2 - k_z^2) (g_R + 2ck^2) S(\mathbf{k}, t). \end{aligned} \quad (9)$$

For the case of steady shear flow, we define the excess viscosity $\Delta\eta = \sigma_{xy}/\dot{\gamma}$, the first normal stress coefficient $\psi_1 = N_1/\dot{\gamma}^2$, and the second normal stress coefficient $\psi_2 = N_2/\dot{\gamma}^2$. For oscillatory shear, we will introduce a complex viscosity later on. However, Eqs. (7)–(9) already involve some assumptions and therefore require comment. Starting from a general Hamiltonian, every term that is free of space derivatives gives an isotropic contribution to the pressure tensor, which is, however, not of interest here. In addition, each term containing space derivatives influences the components of the pressure tensor in a more general way. A Gaussian Hamiltonian yields a tensor that is quadratic in the order parameter field as given in [2,3]. Shear and principal stresses can then be expressed exactly in terms of the quasistatic structure factor. The g_2 term invalidates this simple picture and adds quartic terms in ϕ to the stresses. However, we here propose not to consider these terms in detail but to generalize the Gaussian result in an appropriate way. Instead of the bare interfacial tension g_0 we will calculate the stresses on the basis of a renormalized interfacial tension g_R . In field-theoretical language, this amounts to first determining a loop corrected two-point vertex function with the shear rate set to zero, a task which can be accomplished by standard methods. This dressed two-point function then permits us to construct an effective Gaussian model, formulated in terms of renormalized coefficients or even directly in terms of correlation lengths. One then calculates the shear response of this effective model by use of the functionals (7)–(9). The weak point of such an approach is the neglect of any coupling between the Langevin relaxation dynamics and

the shear term in the evolution equation for the quasistatic structure factor. However, its appropriateness will be demonstrated for low shear rates to the order of one loop below. Physically one can argue that the energies involved in the fluctuation processes that give rise to excess stresses stem from interfacial stretching and bending contributions. Macroscopically observable stresses should then not depend on the very microscopic details of the particular model under consideration but on these effective energy scales.

Under the influence of the shear velocity field (6), in Fourier space the order parameter follows the stochastic evolution equation

$$\begin{aligned} \frac{\partial \phi(\mathbf{k})}{\partial t} &= \dot{\gamma}(t) k_x \frac{\partial}{\partial k_y} \phi(\mathbf{k}) - \Gamma(k) \left[K(k) \phi(\mathbf{k}) \right. \\ &\quad + \frac{\lambda}{6} \int \frac{d\mathbf{k}_1}{(2\pi)^D} \frac{d\mathbf{k}_2}{(2\pi)^D} \phi(\mathbf{k}_1) \phi(\mathbf{k}_2) \phi(\mathbf{k} - \mathbf{k}_1 - \mathbf{k}_2) \\ &\quad + g_2 \int \frac{d\mathbf{k}_1}{(2\pi)^D} \frac{d\mathbf{k}_2}{(2\pi)^D} (|\mathbf{k} - \mathbf{k}_1 - \mathbf{k}_2|^2 + \mathbf{k}_1 \cdot \mathbf{k}_2) \\ &\quad \left. \times \phi(\mathbf{k}_2) \phi(\mathbf{k}_1) \phi(\mathbf{k} - \mathbf{k}_1 - \mathbf{k}_2) \right] + \eta_\phi(\mathbf{k}), \end{aligned} \quad (10)$$

where $K(k) = ck^4 + g_0 k^2 + a_2$ is the bare two-point vertex function. This equation generalizes the result for the pure Gaussian case as given in Ref. [2]. In order to proceed, we approximate the nonlocal terms in Fourier space on a level that has already been successfully used to study fluctuations in a Landau-Ginzburg-Wilson theory of microemulsions [18]. It is also believed to capture essential features of the relaxation process occurring when self-assembly is quenched from the unstructured region of the phase diagram into the structured microemulsion region [4]. The one-loop approximation for the evolution equation of the quasistatic structure factor,

$$S(\mathbf{k}, t) = \langle \phi(\mathbf{k}, t) \phi(-\mathbf{k}, t) \rangle, \quad (11)$$

amounts to applying Wick’s theorem for the Gaussian closure of fourth-order moments, so that

$$\begin{aligned} &\left[\frac{\partial}{\partial t} + 2\Gamma(k) \left[K(k) + g_2 k^2 G_0(t) + \left(\frac{\lambda}{2} G_0(t) + g_2 G_2(t) \right) \right] \right. \\ &\quad \left. - \dot{\gamma}(t) k_x \frac{\partial}{\partial k_y} \right] S(\mathbf{k}, t) \\ &= 2\Gamma(k) T, \end{aligned} \quad (12)$$

where the term in the inner square brackets is the one-loop approximation for the two-point vertex function. For the fully dressed one-loop theory, G_0 and G_2 are defined in terms of the relations

$$G_0(t) = \int \frac{d\mathbf{q}}{(2\pi)^D} S(\mathbf{q}, t), \quad (13)$$

$$G_2(t) = \int \frac{d\mathbf{q}}{(2\pi)^D} q^2 S(\mathbf{q}, t), \quad (14)$$

thereby yielding a self-consistent theory.

STEADY SHEAR

In this section we are concerned with the steady-state solutions of the evolution equation (12) for the quasistatic structure factor. We impose a shear velocity field that is constant in time, having applied in the past, and all transients have vanished. Thus, we here do not consider the kinetic stage where the fluid adapts to the nonequilibrium conditions but assume that the asymptotic regime has been reached where the structure factor is time independent.

Gaussian case: $\lambda = g_2 = 0$ and $\dot{\gamma} = \text{const} \neq 0$

Before dealing with the loop corrections, let us make some comments on the Gaussian case,

$$\left[2\Gamma(k)K(k) - \dot{\gamma}k_x \frac{\partial}{\partial k_y} \right] S(\mathbf{k}) = 2\Gamma(k)T, \quad (15)$$

which has also been treated in our previous paper [2], in part by direct simulation of the Langevin equation for the order parameter. Note that Eq. (15) is an ordinary, linear, first-order differential equation in k_y , so

$$\frac{dS(\mathbf{k})}{dk_y} = A(\mathbf{k})S(\mathbf{k}) - B(\mathbf{k}), \quad (16)$$

with

$$A(\mathbf{k}) = \frac{2\Gamma(k)K(k)}{\dot{\gamma}k_x}, \quad (17)$$

$$B(\mathbf{k}) = \frac{2\Gamma(k)T}{\dot{\gamma}k_x}. \quad (18)$$

In a plane of fixed k_x and k_z , these wave number components merely enter as additional parameters. For physical reasons, we have the boundary conditions $S(-\infty) = S(\infty) = 0$. The given inhomogeneous problem then has the formal solution,

$$S(k_y) = - \int_{-\infty}^{k_y} dk'_y B(k'_y) \exp \left[\int_{k'_y}^{k_y} A(k''_y) dk''_y \right]. \quad (19)$$

The inner integral under the exponential is over a polynomial in k''_y . However, the outer integral cannot be performed by elementary means. Also note that this representation is problematic in the region $k_x \dot{\gamma} \approx 0$, since $A(\mathbf{k})$ and $B(\mathbf{k})$ grow beyond all limits in this case, whereas the original problem (15) has a trivial solution for $k_x \dot{\gamma} = 0$. In the following perturbative treatment, the idea is to write the structure factor as a straightforward power series in the shear rate $\dot{\gamma}$, starting with the equilibrium structure factor as the zero-order term. This approach has been followed in our previous paper [2], and will again be used in connection with the loop corrections later on.

Self-consistent solution for $\lambda, g_2 \neq 0$ but $\dot{\gamma} = 0$

Before we combine the influences of shear and nonlinearities on the solution of Eq. (12), it is useful to consider the role of the latter first. For zero shear, we have

$$\left[K(k) + g_2 k^2 G_0 + \left(\frac{\lambda}{2} G_0 + g_2 G_2 \right) \right] S(\mathbf{k}) = T. \quad (20)$$

As usual, the solution for the structure factor is given by the inverse of the loop-corrected two-point vertex function, the expression in the square brackets. This can be written as

$$S(\mathbf{k}) = \frac{T}{c} \frac{1}{k^4 + gk^2 + a}, \quad (21)$$

where we have introduced the renormalized coefficients,

$$g = \frac{g_0}{c} + \frac{g_2}{c} G_0, \quad (22)$$

$$a = \frac{a_2}{c} + \frac{\lambda}{2c} G_0 + \frac{g_2}{c} G_2. \quad (23)$$

However, we note that the foregoing definitions contain the self-consistent expressions for the loop integrals in terms of the solution (21) itself, requiring

$$\begin{aligned} G_0 &= \int \frac{d\mathbf{q}}{(2\pi)^D} S(\mathbf{q}) = \frac{T}{2\pi^2 c} \int_0^\infty \frac{q^2 dq}{q^4 + gq^2 + a} \\ &= \frac{T}{4\pi c} \frac{1}{\sqrt{2\sqrt{a} + g}}, \end{aligned} \quad (24)$$

$$G_2 = \int \frac{d\mathbf{q}}{(2\pi)^D} q^2 S(\mathbf{q}) = \frac{T}{2\pi^2 c} \int_0^\Lambda \frac{q^4 dq}{q^4 + gq^2 + a} \approx \frac{T\Lambda}{2\pi^2 c}. \quad (25)$$

The second integral is UV divergent in three dimensions and we have had to introduce a cutoff. We leave the equations in this form since a renormalization group treatment is not within the scope of this paper but we hope to comment on this aspect at a later time. The combination of Eqs. (22)–(25) yields a pair of coupled nonlinear equations for the renormalized coefficients g and a ,

$$g = \frac{g_0}{c} + \frac{g_2 T}{4\pi c^2} \frac{1}{\sqrt{2\sqrt{a} + g}}, \quad (26)$$

$$a = \frac{a_2}{c} + \frac{\lambda T}{8\pi c^2} \frac{1}{\sqrt{2\sqrt{a} + g}} + \frac{g_2 T}{2\pi^2 c^2} \Lambda. \quad (27)$$

Equations of this kind have been derived and studied previously in the diagrammatic expansion of the self-energy for the self-consistent treatment of fluctuation effects in microemulsions [18], in connection with relaxation phenomena in self-assembled systems [4], and for large- N models both for growth kinetics [5] and self-assembled fluids [6]. The natural choice for the cutoff Λ is known to be the length of the amphiphile molecule [14]. This given, the nonlinear equations can be solved numerically by fixed-point iteration. It is

more significant to note that we can formulate the results directly in terms of the physical correlation lengths, thereby making direct comparisons to experiment possible. In the disordered region of the phase diagram, the real space correlation function for the bicontinuous microemulsion is given by

$$g(r) = \frac{e^{-r/\xi}}{r} \sin \frac{2\pi r}{d}. \quad (28)$$

The physical correlation lengths ξ and d are computed from the renormalized coefficients according to

$$\frac{d}{2\pi} = \frac{2}{\sqrt{2\sqrt{a}-g}}, \quad (29)$$

$$\xi = \frac{2}{\sqrt{2\sqrt{a}+g}}. \quad (30)$$

The nonlinear couplings λ and g_2 given, we can now eliminate the bare coefficients g_0 and a_2 from the theory,

$$\frac{g_0}{c} = 2 \left[\left(\frac{1}{\xi} \right)^2 - \left(\frac{2\pi}{d} \right)^2 \right] - \frac{g_2 T \xi}{8\pi c^2} \quad (31)$$

$$\frac{a_2}{c} = \left[\left(\frac{1}{\xi} \right)^2 + \left(\frac{2\pi}{d} \right)^2 \right]^2 - \frac{\lambda T \xi}{16\pi c^2} - \frac{g_2 T}{2\pi^2 c^2} \Lambda. \quad (32)$$

Thus, independent of bare coefficients, except for an overall factor, the equilibrium structure factor expressed in terms of the correlation lengths is

$$S(\mathbf{k}) = \frac{T}{c} \left[k^4 + 2 \left[\left(\frac{1}{\xi} \right)^2 - \left(\frac{2\pi}{d} \right)^2 \right] k^2 + \left[\left(\frac{1}{\xi} \right)^2 + \left(\frac{2\pi}{d} \right)^2 \right]^2 \right]^{-1}. \quad (33)$$

Perturbative solution for $\lambda, g_2 \neq 0$ and small $\dot{\gamma} \neq 0$

We now consider the solution of Eq. (12) for low shear and with the nonlinearities present. The procedure relies on a Taylor expansion of the structure factor in the shear rate $\dot{\gamma}$,

$$S(\mathbf{k}) = S_0(\mathbf{k}) + \dot{\gamma} S_1(\mathbf{k}) + \dot{\gamma}^2 S_2(\mathbf{k}) + O(\dot{\gamma}^3). \quad (34)$$

However, in the case of a conserved order parameter, this series is problematic, since we meet infrared (IR) divergences when we attempt to use the resulting structure factor to derive expansions of the rheological coefficients in the shear rate. The reason is that due to conservation, the relaxation dynamics slows down proportionally to k^2 on small wave number scales, whereas the shear term only scales linearly with k_x . On the other hand, a series expansion of the structure factor at least to second order in the shear rate is necessary to obtain analytic estimates for the rheological coefficients at zeroth order. Note also that the loop integrals G_0 and G_2 according to Eqs. (13) and (14) have an expansion in $\dot{\gamma}$ now. We first consider terms in Eq. (12) that are independent of the shear rate. At zero order, we obtain

$$S_0(\mathbf{k}) = \frac{T}{K_R(k)}, \quad (35)$$

where

$$K_R(k) = c[k^4 + gk^2 + a] \quad (36)$$

is the loop-corrected two-point vertex function as already introduced implicitly in Eq. (21) with renormalized coefficients according to Eq. (26) and (27). On the level linear in the shear rate, we must compute $S_1(\mathbf{k})$ from

$$2\Gamma(k)K_R(k)S_1(\mathbf{k}) + 2\Gamma(k) \left[g_2 k^2 G_0^{(1)} + \left(\frac{\lambda}{2} G_0^{(1)} + g_2 G_2^{(1)} \right) \right] S_0(\mathbf{k}) - k_x \frac{\partial S_0(\mathbf{k})}{\partial k_y} = 0, \quad (37)$$

where $G_0^{(1)}$ and $G_2^{(1)}$ denote contributions linear in $\dot{\gamma}$ to the loop integrals. The solution is given by

$$S_1(\mathbf{k}) = - \frac{T}{\Gamma c^2} \frac{k_x k_y (g + 2k^2)}{k^2 (k^4 + gk^2 + a)^3}. \quad (38)$$

Due to the spherical symmetry, the loop corrections vanish on this level, $G_0^{(1)} = G_2^{(1)} = 0$, as can be seen by inserting Eq. (38) into Eqs. (13) and (14). On the level quadratic in the shear rate, we find

$$S_2(\mathbf{k}) = \frac{k_x}{2\Gamma(k)K_R(k)} \frac{\partial S_1(\mathbf{k})}{\partial k_y} + \left[g_2 k^2 G_0^{(2)} + \left(\frac{\lambda}{2} G_0^{(2)} + g_2 G_2^{(2)} \right) \right] S_0(\mathbf{k}). \quad (39)$$

At this stage, the loop integrals $G_0^{(2)}$ and $G_2^{(2)}$ do not vanish. However, the second term in the above sum again has spherical symmetry. Because of the overall factors $(k_x k_y)$, $(k_x^2 - k_y^2)$, and $(k_y^2 - k_z^2)$ in the integrands, this term yields no contribution to the functionals (7)–(9) for the shear stress and the normal stress differences. We do not calculate these corrections to the zero-order loop integrals here and only give the first term in Eq. (39) explicitly,

$$S_2(\mathbf{k}) \approx - \frac{T k_x^2}{2\Gamma^2 c^3 k^4 (k^4 + gk^2 + a)^4} \left[(g + 2k^2) - 2k_y^2 \frac{g(k^4 + gk^2 + a) + 3k^2(g + 2k^2)^2}{k^2(k^4 + gk^2 + a)} \right]. \quad (40)$$

Symmetry considerations again reveal the first term in the square brackets combined with the factor $(k_x^2 - k_y^2)$ in Eq. (8) gives rise to a nonzero first normal stress difference, and, similarly, the second term to a nonzero second normal stress difference. Also note the overall factors k^{-2} in Eq. (38) and k^{-4} in Eq. (40) that indicate the buildup of IR divergences as mentioned earlier.

The origin of the IR divergences can be traced back to the conservative nature of the used model. Conservation of matter results in the slowing down of shear deformations on

large spatial or small wave number scales. As noted most clearly in Ref. [12], Eq. (12) is a singularly perturbed differential equation with a boundary layer at $k_x=0$. This feature stems from the fact that the small quantity, $\dot{\gamma}k_x$, multiplies the highest derivative in the equation. We therefore have to expect a qualitative change in the properties of the solution between $\dot{\gamma}k_x \rightarrow 0$ and $\dot{\gamma}k_x = 0$. Any regular perturbation series like Eq. (34) gives the so-called outer solution which is a bad approximation in the inner region. The inner solution which is valid in the boundary layer cannot be calculated by use of regular perturbation methods [19]. On the other hand, the dominant contributions when calculating the rheological coefficients come from a region in wave number space which is bounded away from zero [2]. This means that we are obviously in a somewhat lucky situation, since the functionals (7)–(9) for the rheological coefficients involve integration over all wave number space which smears the error due to the boundary layer somewhat. Therefore we do not want to go so far as Ref. [12] and declare that there is no linear response at all, because we believe the scaling forms (41)–(43) will be useful when analyzing weak shear experiments.

From what has been computed so far, we see that the loop corrections will not have a direct influence on the values of the rheological coefficients, in the sense that $G_0^{(1)}$ and $G_2^{(1)}$ are zero and $G_0^{(2)}$ and $G_2^{(2)}$ do not contribute to the functionals (7)–(9) due to symmetry. The only effect that changes the result compared to the Gaussian case is the modification of the zero-order structure factor caused by the appearance of the dressed two-point vertex function according to Eq. (35). The formulas derived for the Gaussian case in our previous paper [2] therefore remain valid if we use them in scaling form and expressed in terms of the physical correlation lengths. These we either simply prescribe or compute according to Eqs. (29) and (30) with the one-loop renormalized coefficients g and a given self-consistently by Eqs. (26) and (27). This is equivalent to first computing the loop corrections for zero shear, then constructing an effective Gaussian model with Eq. (36) as the vertex function, and finally computing its shear response by use of the functionals (7)–(9). This establishes the approach already discussed in the Introduction. For comparison, we give the expressions for the excess viscosity and the first normal stress coefficient as already derived in [2] and present a new formula for the second normal stress coefficient,

$$\Delta \eta = \frac{T \xi^3}{240 \pi \Gamma c} f_1(\alpha), \quad (41)$$

$$f_1(\alpha) = \frac{\pi^2 + \alpha^2}{4 \pi^2 + \alpha^2},$$

$$\psi_1 = \frac{T \xi^5 d^4}{3840 \pi \Gamma^2 c^2} f_2(\alpha),$$

$$f_2(\alpha) = \frac{32 \pi^6 + 32 \pi^4 \alpha^2 + 2 \pi^2 \alpha^4 + 7 \alpha^6}{(4 \pi^2 + \alpha^2)^5}, \quad (42)$$

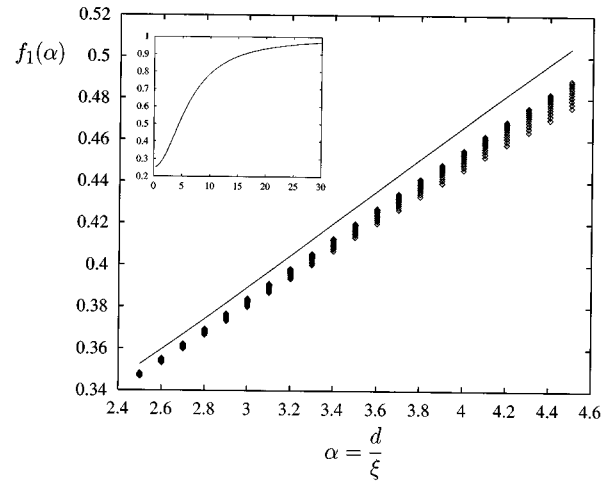


FIG. 1. Scaling function $f_1(\alpha)$ according to Eq. (41) and numerical data for the excess viscosity. The main figure is restricted to the values of α observed in experiments, the inset shows a larger part of the scaling function. The data points come from numerical solutions of Eq. (12) for different values of α and d between $d=4.5$ and $d=5.5$ ($\lambda = g_2 = 1$).

$$\psi_2 = \frac{T \xi^5 d^4}{53760 \pi \Gamma^2 c^2} f_3(\alpha),$$

$$f_3(\alpha) = \frac{368 \pi^6 + 376 \pi^4 \alpha^2 + 51 \pi^2 \alpha^4 + 63 \alpha^6}{(4 \pi^2 + \alpha^2)^5}. \quad (43)$$

Here $\alpha = d/\xi$ is the ratio of the correlation lengths, which, practically, varies between 2.6 and 4.5 in experiments [20]. The relation (41) has first been derived in [3] for the pure Gaussian case from the zero-frequency limit of the complex shear modulus, which describes the stress response to oscillatory shear, see below.

The scaling function $f_1(\alpha)$ for the excess viscosity and results from numerical solutions of equation (12) have been plotted in Fig. 1. In this and the two following figures, the scaling laws have been tested numerically for $\alpha=2.5$ to $\alpha=4.5$. There is apparently a dispersion of the scaling data for increasing α which can be explained as follows. The functional (7) for the shear stress σ_{xy} receives its essential contribution from a shell of wave numbers somewhat higher than those corresponding to the maximum of the structure factor. Obviously, there is an error due to the truncation of the numerical solution in wave number space. For higher values of α , the structure factor shows the tendency to spread out to larger $|\mathbf{k}|$. Therefore this error increases with fixed numerical truncation for larger values of α . The comparison between the scaling function $f_2(\alpha)$ and numerical data in Fig. 2 for the first normal stress coefficient shows dispersion for low values of α . This happens because the functional (8) for the first normal stress difference receives its main contribution from the low wave number region. Working with a fixed numerical grid, this region is somewhat more poorly represented for large values of d and ξ , resulting in small α

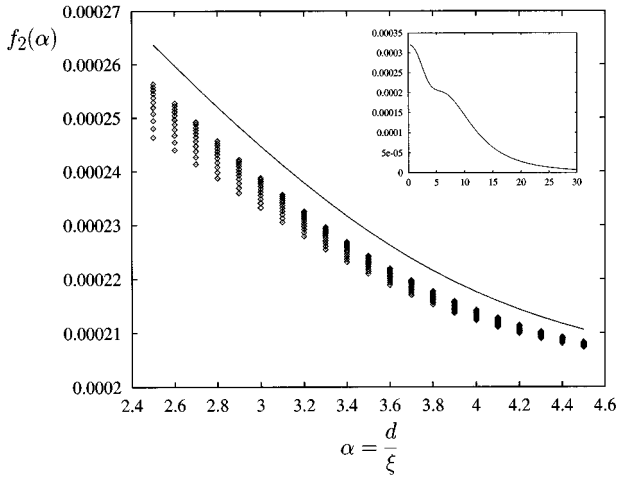


FIG. 2. Scaling function $f_2(\alpha)$ according to Eq. (42) and numerical data for the first normal stress coefficient. The main figure is restricted to the values of α observed in experiments, the inset shows a larger part of the scaling function. The data points come from numerical solutions of Eq. (12) for different values of α and d between $d=4.5$ and $d=5.5$ ($\lambda=g_2=1$).

where the structure factor concentrates its intensity at the origin. The same remarks apply to the numerical data for the second normal stress coefficient compared to the scaling function $f_3(\alpha)$ in Fig. 3. Note that the model considered here predicts a negative second normal stress coefficient, which is in accordance with general experimental experience nowadays [17,21].

For completeness we mention that without meeting IR divergence, we can also compute the derivative of the excess viscosity with respect to the shear rate at the origin,

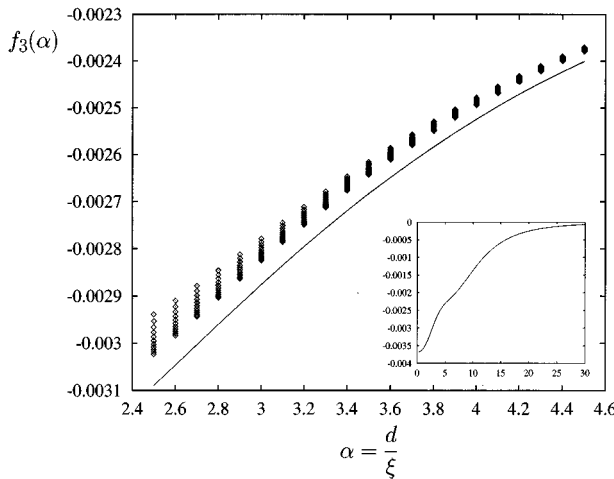


FIG. 3. Scaling function $f_3(\alpha)$ according to Eq. (43) and numerical data for the second normal stress coefficient. The main figure is restricted to the values of α observed in experiments, the inset shows a larger part of the scaling function. The data points come from numerical solutions of Eq. (12) for different values of α and d between $d=4.5$ and $d=5.5$ ($\lambda=g_2=1$).

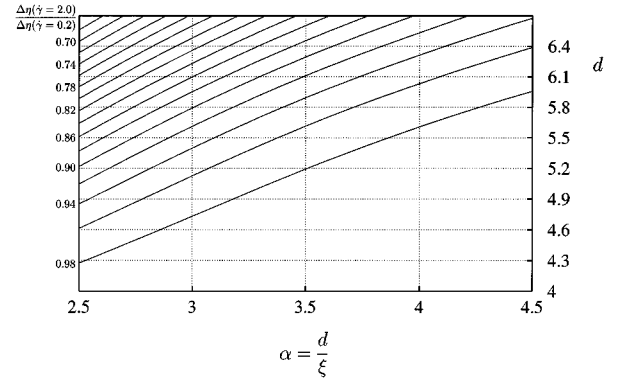


FIG. 4. The decrease of the excess viscosity with increasing shear rate, a signature of non-Newtonian behavior. To obtain this figure, Eq. (12) was first solved numerically for a shear rate of $\dot{\gamma}_1=0.2$, and then for $\dot{\gamma}_2=2.0$. The figure shows the contours of the ratio between the two excess viscosities determined in this way.

$$\frac{\partial \Delta \eta}{\partial \dot{\gamma}^2} = - \frac{T \xi^9 d^6}{6881280 \pi \Gamma^3 c^3} f_4(\alpha),$$

$$f_4(\alpha) = \frac{1}{(4\pi^2 + \alpha^2)^9} [71680\pi^{12} + 199680\pi^{10}\alpha^2 + 271872\pi^8\alpha^4 + 262912\pi^6\alpha^6 + 327672\pi^4\alpha^8 - 207948\pi^2\alpha^{10} + 42757\alpha^{12}]. \quad (44)$$

The derivative is less than zero, which indicates shear thinning. Corresponding expressions for the normal stress coefficients cannot be derived due to IR divergence of the integrals.

Non-Newtonian behavior

The perturbative solutions computed so far are valid only for small values of the shear rate. Thinking in terms of a series expansion of the rheological coefficients in $\dot{\gamma}$, the results (41)–(43) represent the zero-order terms at $\dot{\gamma}=0$. However, because of infrared divergences in the conservative

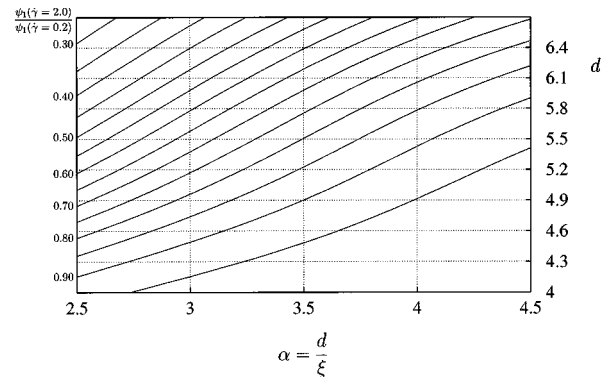


FIG. 5. As expected from the result for the viscosity, the normal stress coefficients are shear rate dependent, too. This is documented here for ψ_1 . The figure shows the contours of the ratio between two values of the first normal stress coefficient obtained for increasing shear in just the same way as the data for the viscosity in the previous figure.

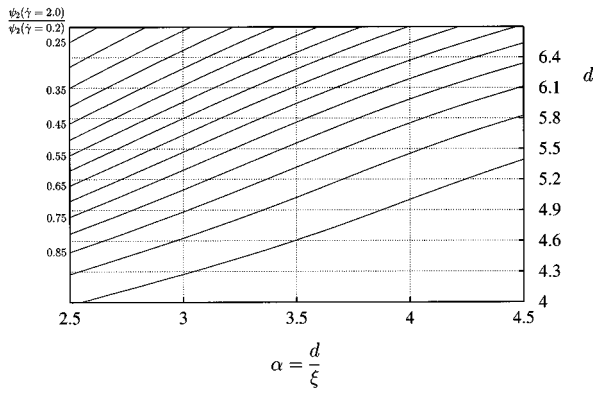


FIG. 6. The shear rate dependency of the second normal stress coefficient. The figure shows the contours of the ratio between two values of the second normal stress coefficient obtained in just the same way as the data for the two previous figures.

case, it is not clear whether an ordinary power series expansion for the rheological coefficients can be devised at all. Before more powerful analytical methods have been found, a possible way out if this difficulty is to obtain the structure factor by numerical solution of Eq. (12) and to compute the rheological coefficients by numerical integration of Eqs. (7)–(9). We have followed this approach and present some results in Figs. 4–7. In general, we observe that all rheological coefficients decrease with increasing shear rate.

To obtain Fig. 4, Eq. (12) was first solved numerically for a shear rate of $\dot{\gamma}_1=0.2$, and then for $\dot{\gamma}_2=2.0$. The figure shows the contours of the ratio $\Delta\eta_2/\Delta\eta_1$ between the two excess viscosities determined in this way. This ratio is always less than one, the fluid behaves shear-thinning. Furthermore, the shear-thinning effect becomes stronger in the highly structured region, that is for large values of d and even larger ones of ξ resulting in small values of α . In Fig. 5 we plotted the contours of the ratio between two values for the first normal stress coefficient obtained for increasing shear in just the same way as the data for the viscosity in Fig. 4. The shear-rate dependency of the normal stress coefficients is found to be stronger than that for the excess viscosity. Again, this effect becomes more pronounced in the highly structured region. Figure 6 then shows the behavior of the second normal stress coefficient. The strong shear-rate dependency and the small absolute magnitude of ψ_2 from the overall numerical factor in Eq. (43) will it make difficult to capture this quantity experimentally.

A sequence of slices through the structure factor in the plane $k_z=0$ for increasing moderate values of the shear rate $\dot{\gamma}$ can be seen in Fig. 7. The above perturbative analytical treatment is successful up to $\dot{\gamma}\approx 1$ ($\Gamma=c=1$). Here the structure factor shows an ellipsoidal deformation with respect to its equilibrium appearance. For higher values of the shear rate, one observes that the intensity on the maximum ring varies significantly. Finally the structure factor concentrates intensity in two regions with finite k_y and small k_x corresponding to elongated structures in the x direction induced by the shear velocity field. At present we possess no analytical procedure for this regime.

Scaling behavior for large shear rates

Common shear-thinning fluids often show a power law for the viscosity, $\eta\sim\dot{\gamma}^n$, which extends over several decades

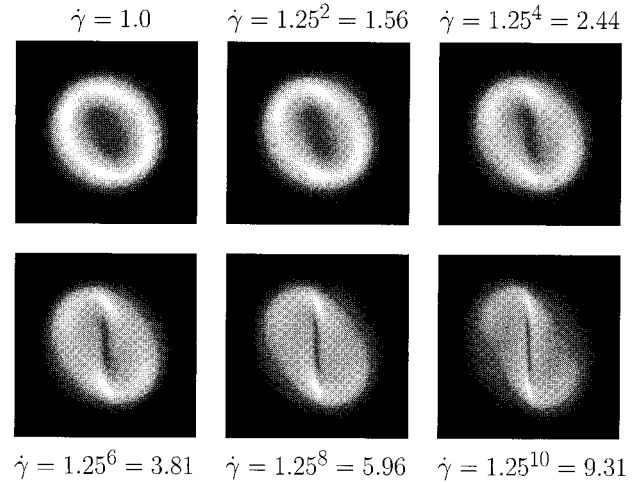


FIG. 7. Sequence of slices through the structure factor in the plane $k_z=0$. For increasing moderate values of the shear rate $\dot{\gamma}$, the pictures are based on the numerical solution of Eq. (12). For $\dot{\gamma}=0$ and ξ and α and $\alpha=d/\xi$ given, the ring of maxima is at wave number $k^2=(1/\xi)^2[(2\pi/\alpha)^2-1]$.

of the shear rate [17,21]. Because the shear stress is then given by $\sigma_{xy}=\eta\dot{\gamma}\sim\dot{\gamma}^{n+1}$, the exponent n must be greater than -1 for physical stability. It is now of interest whether the model considered here leads to such an extended range of shear thinning. Unfortunately, this is not the case. As expected we will find that the model is dominated by the derivative term, $\dot{\gamma}k_x(\partial/\partial k_y)S(\mathbf{k})$ in Eq. (12), at large values for the shear rate, and any signature of the Hamiltonian vanishes asymptotically. To see this, we consider the large- $\dot{\gamma}$ behavior of the steady state structure factor $S(\mathbf{k})$ computed from

$$\left[2\Gamma(k)K_R(k)-\dot{\gamma}k_x\frac{\partial}{\partial k_y}\right]S(\mathbf{k})=2\Gamma(k)T. \quad (45)$$

We use the loop-corrected vertex function $K_R(k)$ here, but this is not essential for the argument. It should be noted that the structure factor for $k_x=0$ is not affected by the shear at all. Now we first restrict our attention to a neighborhood in \mathbf{k} space next to the plane $k_x=0$ and consider the situation where $k_x\approx 0$ but $\dot{\gamma}k_x=\text{const}$ for $\dot{\gamma}\rightarrow\infty$. The transformation: $\dot{\gamma}\rightarrow s\dot{\gamma}$, $k_x\rightarrow k_x/s$, $s>1$ leaves $|\mathbf{k}|^2$ essentially unchanged, since $k_x\approx 0$. Equation (45) is therefore approximately invariant in the given region under the transformation, which leads to the relation

$$S\left(\frac{k_x}{s}, s\dot{\gamma}\right)=S(k_x, \dot{\gamma}). \quad (46)$$

For increasing shear rate, Eq. (46) describes the behavior of the structure factor in a shrinking region in wave number space. Now let us investigate the consequence of this relation for the shear stress. If we use it in the expression (7), we find by a simple substitution $\sigma_{xy}(s\dot{\gamma})=(1/s^2)\sigma_{xy}(\dot{\gamma})$, and therefore $\sigma_{xy}\sim\dot{\gamma}^{-2}$ or equivalently $\Delta\eta\sim\dot{\gamma}^{-3}$. We also find $N_1\sim\dot{\gamma}^{-1}$ and $N_2\sim\dot{\gamma}^{-1}$, which means $\psi_1\sim\dot{\gamma}^{-3}$ and $\psi_2\sim\dot{\gamma}^{-3}$.

However, because for increasing shear rate this behavior stems from a region of shrinking integration measure in \mathbf{k} space, we must also consider the behavior of the structure

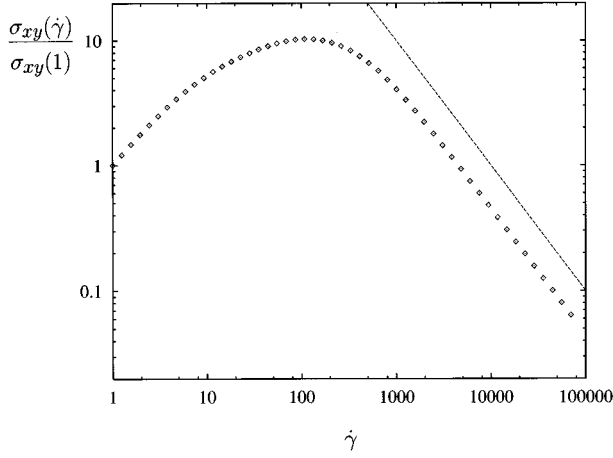


FIG. 8. Behavior of the shear stress for large values of the shear rate $\dot{\gamma}$ confirming the scaling result Eq. (47) presented in the text. The dashed line has a slope of -1 .

factor well away from the plane $k_x=0$. Now for some finite value of k_x , we can always find some large enough value for the shear rate such that the contribution coming from the Hamiltonian in Eq. (45) becomes irrelevant and the right-hand side is balanced essentially by the derivative term. This implies the scaling $S(\mathbf{k}) \sim \dot{\gamma}^{-1}$ and simply gives $\sigma_{xy} \sim \dot{\gamma}^{-1}$, $N_1 \sim \dot{\gamma}^{-1}$, and $N_2 \sim \dot{\gamma}^{-1}$, and therefore $\Delta\eta \sim \dot{\gamma}^{-2}$, whereas $\psi_1 \sim \dot{\gamma}^{-3}$ and $\psi_2 \sim \dot{\gamma}^{-3}$ as before. From the two scaling cases considered, we expect for very high shear rates the slower laws to survive. This argument applies especially for the excess viscosity. We expect the final laws

$$\sigma_{xy} \sim \dot{\gamma}^{-1}, \quad \Delta\eta \sim \dot{\gamma}^{-2}, \quad (47)$$

which come from the scaling away from the plane $k_x=0$ and are independent of the form of the Hamiltonian. The normal stress coefficients are expected to decay with $\dot{\gamma}^{-3}$.

Figure 8 shows the behavior of the shear stress for large values of the shear rate and confirms the scaling argument just given. In interpreting this result, one should, however, remember that $\Delta\eta$ is the excess viscosity and σ_{xy} , as defined in this paper, is the excess stress caused by the fluids internal fluctuating structure. The full stress is given by this contribution and the one coming from the background viscosity η_0 in Eq. (3). The seemingly paradoxical decrease of the excess stress for large shear rate does not necessarily mean an instability of the model as long as the Newtonian background viscosity is the dominant contribution. The decrease merely reflects the certainly overestimated adaption of the fluids internal interfacial structure to the preferred direction of the imposed flow. This can be inferred from Fig. 9, which shows the structure factor for high shear rates. It degenerates into a strip of decreasing width along the k_y axis. The pictures represent cuts for $k_z=0$, but there is a rotational symmetry with respect to the k_x axis.

OSCILLATORY SHEAR

As the simplest time-dependent situation, which is nevertheless of significant experimental relevance especially when probing viscoelastic properties, we now consider the shear stress induced by oscillatory shear flow, where

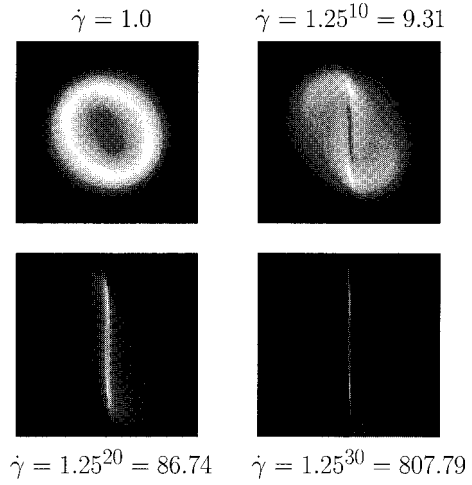


FIG. 9. The structure factor in the plane $k_z=0$ for high values of the shear rate. The structure factor degenerates into a strip of decreasing width along the k_y axis. Asymptotically, there is a rotational symmetry with respect to the k_x axis. For $\dot{\gamma}=0$ and ξ and $\alpha=d/\xi$ given, the ring of maxima is at wave number $k^2 = (1/\xi)^2[(2\pi/\alpha)^2 - 1]$.

$$\dot{\gamma}(t) = \dot{\gamma}_0 \cos(\omega t). \quad (48)$$

Again we are not interested in any transient behavior but suppose that a steady, oscillatory stress response has built up. In the previous section, we used the linear term in a $\dot{\gamma}$ expansion of the shear stress to compute the excess viscosity. Accordingly, we now assume that we are in the oscillatory linear response regime. It is then customary to introduce the complex shear modulus $G^*(\omega)$ and to write

$$\sigma_{xy}(t) = \text{Re} \left[\frac{1}{i\omega} G^*(\omega) \dot{\gamma}_0 e^{i\omega t} \right]. \quad (49)$$

Now $G^*(\omega) = G'(\omega) + iG''(\omega)$, and the shear stress is explicitly given by

$$\sigma_{xy} = \frac{\dot{\gamma}_0}{\omega} [G'(\omega) \sin(\omega t) + G''(\omega) \cos(\omega t)]. \quad (50)$$

The contribution proportional to the storage modulus $G'(\omega)$ is in phase with the strain, whereas the one proportional to the loss modulus $G''(\omega)$ is in phase with the shear rate. However, the formulation using the complex shear modulus is more appropriate if we originally prescribe not the shear rate but the strain. Here we prefer to work with a complex viscosity, $\eta^*(\omega) = \eta'(\omega) - i\eta''(\omega)$, and to use the representation

$$\begin{aligned} \sigma_{xy}(t) &= \text{Re}[\eta^* \dot{\gamma}_0 e^{i\omega t}] \\ &= \dot{\gamma}_0 [\eta'(\omega) \cos(\omega t) + \eta''(\omega) \sin(\omega t)]. \end{aligned} \quad (51)$$

The dynamic viscosity $\eta'(\omega)$ multiplies the portion of the response which is in phase with the shear rate, whereas the dynamic elasticity $\eta''(\omega)$ gives the stress response in phase with the strain. The connection to the complex shear modulus is given by $G' = \omega\eta''$ and $G'' = \omega\eta'$. Another common representation of the stress response is, of course,

$$\sigma_{xy}(t) = A(\omega) \sin[\omega t + \phi(\omega)]. \quad (52)$$

The connection between Eqs. (51) and (52) is given by

$$A = \dot{\gamma}_0 \sqrt{\eta'^2 + \eta''^2} \quad (53)$$

and

$$\sin \phi = \frac{\eta'}{\sqrt{\eta'^2 + \eta''^2}}, \quad (54)$$

$$\cos \phi = \frac{\eta''}{\sqrt{\eta'^2 + \eta''^2}}. \quad (55)$$

The phase angle $\phi(\omega)$ has been introduced with reference to the time-dependency of the strain. Therefore, if $\phi > 0$, the stress anticipates the strain, and if $\phi < 0$, the stress follows the strain. Pure viscous behavior corresponds to $\phi = \pi/2$, pure elastic behavior to $\phi = 0$.

We now solve Eq. (12) with a shear rate given by Eq. (48). Loop corrections arising from the nonlinear terms will lead to mode coupling. However, we will not treat the case of strong coupling here. In that case the assumption of a linear response without frequency shift would no longer be satisfied. On the other hand, we have seen previously that non-Newtonian effects like a shear-rate-dependent viscosity and normal stress differences are already present at the Gaussian level. They certainly do not depend on specific higher-order terms in the Hamiltonian. It therefore does not come as a surprise that we will be able to establish viscoelastic behavior by use of an effective Gaussian model as introduced in the previous section. To be specific, the first improvement with regard to the bare Gaussian treatment consists in solving

$$\left[\frac{\partial}{\partial t} + 2\Gamma(k)K_R(k) - \dot{\gamma}(t)k_x \frac{\partial}{\partial k_y} \right] S(\mathbf{k}, t) = 2\Gamma(k)T, \quad (56)$$

where $K_R(k)$ is the loop-corrected two-point vertex function as defined above in Eq. (36). In the linear response regime,

$$S(\mathbf{k}, t) = S_0(\mathbf{k}) + \text{Re}[\dot{\gamma}_0 S_1(\mathbf{k}, \omega) e^{i\omega t}]. \quad (57)$$

The background part of the structure factor is again given by

$$S_0(\mathbf{k}) = \frac{T}{K_R(k)}, \quad (58)$$

and the time-dependent correction is easily found to be

$$S_1(\mathbf{k}, \omega) = \frac{k_x}{i\omega + 2\Gamma(k)K(k)} \frac{\partial S_0(k)}{\partial k_y}. \quad (59)$$

We split into real and imaginary part,

$$S_1(\mathbf{k}, \omega) = S'_1(\mathbf{k}, \omega) - iS''_1(\mathbf{k}, \omega) \quad (60)$$

and obtain

$$S'_1(\mathbf{k}, \omega) = \frac{2k_x \Gamma(k) K(k)}{\omega^2 + 4\Gamma^2(k) K^2(k)} \frac{\partial S_0(k)}{\partial k_y}, \quad (61)$$

$$S''_1(\mathbf{k}, \omega) = \frac{k_x \omega}{\omega^2 + 4\Gamma^2(k) K^2(k)} \frac{\partial S_0(k)}{\partial k_y}. \quad (62)$$

We insert into the functional (7) for the shear stress,

$$\sigma_{xy}(t) = - \int \frac{d\mathbf{k}}{(2\pi)^D} k_x k_y (g_R + 2ck^2) [S_0(k) + \text{Re}[(S'_1(\mathbf{k}, \omega) - iS''_1(\mathbf{k}, \omega)) \dot{\gamma}_0 e^{i\omega t}]]. \quad (63)$$

Comparison with Eq. (51) then results in the identifications

$$\eta'(\omega) = - \int \frac{d\mathbf{k}}{(2\pi)^D} k_x k_y (g_R + 2ck^2) S'_1(\mathbf{k}, \omega), \quad (64)$$

$$\eta''(\omega) = - \int \frac{d\mathbf{k}}{(2\pi)^D} k_x k_y (g_R + 2ck^2) S''_1(\mathbf{k}, \omega). \quad (65)$$

We introduce a normalized frequency,

$$\Omega = \frac{\omega}{\Gamma c}, \quad (66)$$

carry out the angular integrals in Eqs. (64) and (65), and arrive at

$$\eta'(\omega) = \frac{T}{15\pi^2 \Gamma c} \int_0^\infty dk \times \frac{2k^8 (g + 2k^2)^2}{[\Omega^2 + 4k^4 (k^4 + gk^2 + a)^2][k^4 + gk^2 + a]}, \quad (67)$$

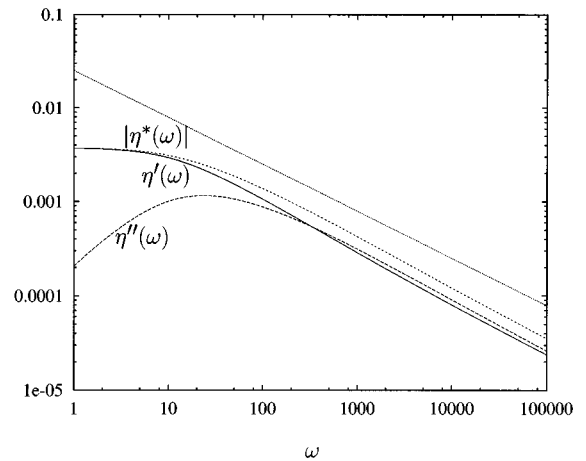


FIG. 10. The development of the complex viscosity for large values of the shear rate frequency ω . The curves for $\eta'(\omega)$, $\eta''(\omega)$, and $|\eta^*(\omega)|$ have been obtained by numerical integration of Eqs. (67) and (68). They confirm the asymptotic results (71) and (72). The straight line has a slope of $-\frac{1}{2}$.

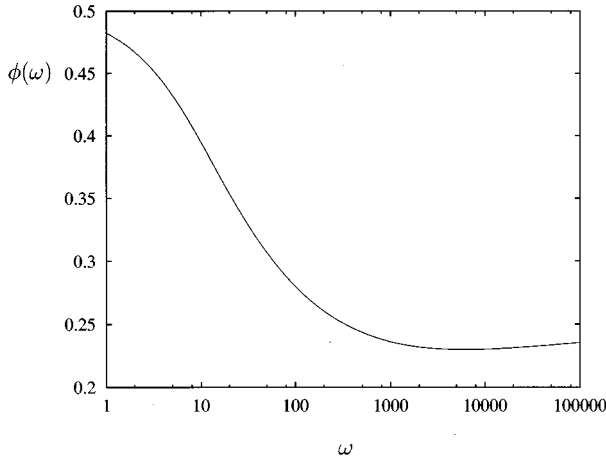


FIG. 11. The development of the phase angle $\phi(\omega)$ in units of π of the stress response for large values of the shear rate frequency ω as obtained by numerical integration of Eqs. (67) and (68). The asymptotic result (72), $\phi(\omega) \rightarrow \pi/4$ ($\omega \rightarrow \infty$) is confirmed. Note, however, that $\phi(\omega)$ approaches the asymptotic value from below, because the fluid is slightly more elastic than viscous, $\eta''(\omega) > \eta'(\omega)$, for large ω .

$$\eta''(\omega) = \frac{T}{15\pi^2\Gamma c} \int_0^\infty dk \times \frac{\Omega k^6 (g + 2k^2)^2}{[\Omega^2 + 4k^4(k^4 + gk^2 + a)^2][k^4 + gk^2 + a]^2}. \quad (68)$$

From this we see that $\eta'(\omega)$ and $\eta''(\omega)$ are non-negative, as could be anticipated from stability considerations, and the phase angle can simply be computed from

$$\tan\phi(\omega) = \frac{\eta'(\omega)}{\eta''(\omega)}. \quad (69)$$

For arbitrary ω , the expressions for η' and η'' were finally evaluated by numerical integration. However, the asymptotic behavior for $\omega \rightarrow \infty$ can be addressed if we use the substitution

$$\kappa = \frac{k}{\Omega^{1/6}}. \quad (70)$$

For both integrals, the limiting expressions coincide,

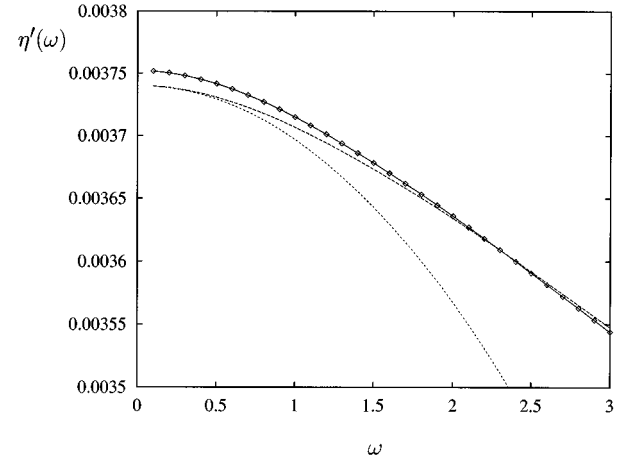


FIG. 12. The real part of the dynamic viscosity according to Eq. (51) obtained by numerical ADI solution of Eq. (56). Also shown in the figure are the result from the numerical integration of Eq. (67) (dashed line) and the parabolic approximation based on Eqs. (41) and (75) (dotted line).

$$\eta'(\omega) = \eta''(\omega) = \frac{T}{45\pi\Gamma c} \Omega^{-1/2} = \frac{T}{45\pi} (\Gamma c \omega)^{-1/2} (\omega \rightarrow \infty). \quad (71)$$

This means that we will find a small stress response with a phase shift in the middle between shear rate and strain,

$$\sigma_{xy}(t) = \frac{\sqrt{2}T\dot{\gamma}_0}{45\pi} (\Gamma c \omega)^{-1/2} \sin\left(\omega t + \frac{\pi}{4}\right). \quad (72)$$

These predictions have been checked by numerical integration of Eqs. (67) and (68). The results for $\eta'(\omega)$, $\eta''(\omega)$, and $|\eta^*(\omega)|$ are shown in Fig. 10, the result for the phase angle $\phi(\omega)$ in Fig. 11. At the other extreme, for small ω , a Taylor expansion is valid. At $\omega=0$, the dynamic viscosity $\eta'(0)$ is identical with the steady state excess viscosity $\Delta\eta$ as given in (41), and the dynamic elasticity $\eta''(0)$ is zero from (68). In addition, we obtain the derivatives

$$\frac{\partial^2 \eta'}{\partial \omega^2} (\omega=0) = -\frac{T}{60\pi^2\Gamma c} \int_0^\infty dk \frac{(g+2k^2)^2}{(k^4+gk^2+a)^5}, \quad (73)$$

$$\frac{\partial \eta''}{\partial \omega} (\omega=0) = \frac{T}{60\pi^2\Gamma c} \int_0^\infty dk \frac{k^2(g+2k^2)^2}{(k^4+gk^2+a)^4}. \quad (74)$$

The integrals can be carried out using the calculus of residues with the result

$$\frac{\partial^2 \eta'(\omega)}{\partial \omega^2} = -\frac{Td^8\xi^7}{122880\pi\Gamma c} f_5(\alpha),$$

$$f_5(\alpha) = \frac{1280\pi^{10} + 3328\pi^8\alpha^2 + 4448\pi^6\alpha^4 + 6448\pi^4\alpha^6 - 4147\pi^2\alpha^8 + 858\alpha^{10}}{(4\pi^2 + \alpha^2)^9}, \quad (75)$$

$$\frac{\partial \eta''(\omega)}{\partial \omega} = \frac{Td^4\xi^5}{7680\pi\Gamma c} f_2(\alpha),$$

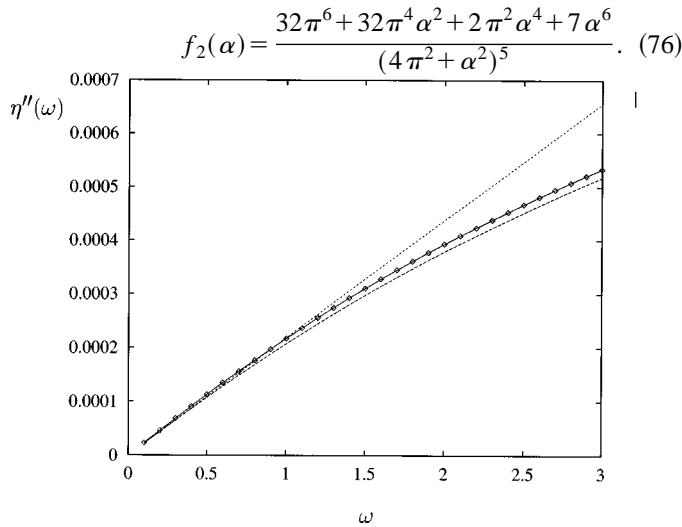


FIG. 13. The imaginary part of the dynamic viscosity according to Eq. (51) from the numerical ADI solution of Eq. (56). Also shown are the result from the numerical integration of Eq. (68) (dashed line) and the linear approximation based on Eq. (76) (dotted line).

Here again we meet the scaling function $f_2(\alpha)$ introduced in Eq. (42).

The behavior of the complex viscosity for small values of the shear frequency ω has been summarized in Figs. 12–15. The data have been obtained for $\Gamma = c = \lambda = g_2 = 1$, $d = 5$, and $\xi = 2$ ($\alpha = 5/2$). We see that in the double limit of small shear rate $\dot{\gamma}_0$ and small frequency ω , the situation is well described by the perturbative treatment given above.

SOME COMPUTATIONAL REMARKS

Many results in this paper have been obtained or were at least checked by the numerical solution of the one-loop equation (12) for the structure factor. We now want to dis-

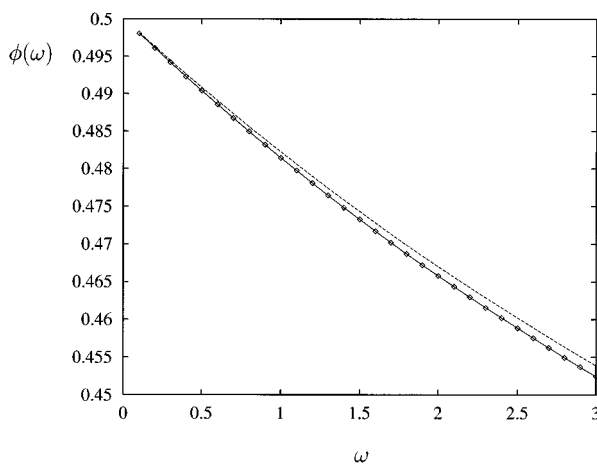


FIG. 14. Phase angle according to Eq. (69) in units of π . Also shown the result based on numerical integration of Eqs. (67) and (68) (dashed line). For low frequencies, the shear response of the systems is nearly that of a liquid. For increasing frequency, the phase angle decreases, indicating that the self-assembled structures give rise to viscoelastic behavior.

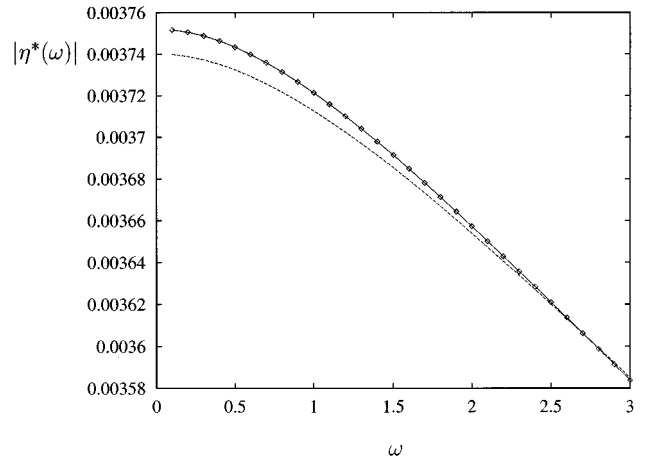


FIG. 15. The modulus of the dynamic viscosity, as obtained from the numerical solution of Eq. (56) and numerical integration of Eqs. (67) and (68) (dashed line).

cuss some ideas used in the numerical schemes. The equation was solved on a DEC Alpha system, Model 2100 4/275. We did not use a parallel computer here, but quite a fast serial machine with appreciable core memory. We exploited the symmetry under the replacement $\mathbf{k} \rightarrow -\mathbf{k}$, which allows us to reduce the problem size by a factor of 4.

The first idea to compute the steady-state solution for the structure factor under shear is to accurately compute the kinetic regime after the shear has switched on, starting with the structure factor at equilibrium. This requires correct wave number and time discretization. However, the broad spectrum of the operator $2\Gamma(k)K_R(k)$ makes this difficult. One would have to use a very small time step, resulting in a prohibitively large number of iteration steps to reach the steady state result.

This problem can be met with a Fourier accelerated relaxation dynamics [22]. Here we use an appropriately weighted time step,

$$\Delta t \mapsto \frac{\Delta t}{K_R(k)(1 + \Gamma(k))}. \quad (77)$$

Large wave number components now relax with the same effective speed as the small ones. The relaxation process does not reflect any real physical evolution, but the steady-state result is unchanged.

The next idea is to replace any relaxation method by a direct linear solver. The matrix formulation of Eq. (12) arising from finite difference discretization amounts to solving a large number of tridiagonal systems coming from the derivative with respect to k_y . These problems are parametrized by the wave number components k_x and k_z . Using the approximate boundary condition $S(\mathbf{k})=0$ for the limiting k_y , these tridiagonal systems can be readily solved by standard methods. We have found this approach to compute the steady-state solution is the most efficient one.

In the case of oscillatory shear one could first think of integrating Eq. (12) in time until some steady response is reached. However, the same remarks as for the accurate time

integration to reach a time-independent steady-state apply. We have applied another approach and exploited the large core memory of our computer to run a full four-dimensional simulation with periodic boundary conditions in the time direction. Now again we have a choice. Either we can implement an artificial relaxation dynamics where the relaxation coordinate no longer corresponds to any physical dimension. Or, corresponding to the direct solution of the time-independent steady-state problem, we can use an alternating-directions implicit method with respect to $\partial/\partial k_y$ and $\partial/\partial t$. This takes a few iteration loops to converge, but gives us the structure factor in a number of time slices over one period of the shear input.

In the methods involving the solution of a set of linear equations, we of course need some additional relaxation iterations to implement the loop corrections. We compute the loop integrals on the basis of the current result for the structure factor and use these values in the next instance of the iteration process. Doing so, we did not have any convergence problems for reasonable values of the problem parameters and appropriate \mathbf{k} -space discretization.

CONCLUSION

The special nature of the shear problem considered here stems from the fact that the shear term is a product of a coordinate function and a gradient operator, both in real space and in Fourier space. On transformation to Fourier space, the associated coordinate directions merely exchange their roles. The appearance of such mixed terms is not shared by common Landau-Ginzburg models, and shear flow is a simple representative of a whole class of problems that involve composite terms of this kind. Others will arise if the order parameter field is subject to other deformations such as elongational flow.

The inclusion of non-Gaussian terms has been accomplished here in a two-stage process. We first used standard methods from statistical field theory to compute the dressed two-point vertex function for zero shear. This vertex function was then used to set up an effective Gaussian model. Its stress response could be computed from the functionals which were readily derived for the Gaussian case. Doing so we neglected the effect of the shear term on mode coupling. However, the validity of the approach could be demonstrated perturbatively for small shear rate. Central results of the paper include the scaling forms for the rheological coefficients under weak shear. The existence of nonzero normal stress differences already indicates the non-Newtonian nature of self-assembly.

Formally due to IR divergences, which indicate however the singular nature of the problem, the information that can be gained by Taylor expansions in the shear rate is limited. We have therefore computed the nonequilibrium structure factor numerically to further study the shear-rate dependence of the rheological coefficients. We found shear thinning and a positive first as well as a negative second normal stress coefficient for all values of the shear rate. For increasing shear, both coefficients approach zero.

For oscillatory shear, viscoelastic behavior was established. In a first linear response approximation for low frequency, the dynamic elasticity increases linearly. Asymptoti-

cally the dynamic viscosity and elasticity approach the same function of the shear frequency, and the phase of the stress response lies in the middle between shear and strain.

Integral representations like Eq. (19) for the steady quasistatic structure factor under shear have been reported previously. One either starts from the steady-state problem and uses the variation of parameters technique or equivalent methods [12] to derive an integral representation for the solution of the emerging linear first-order differential equation. Or one treats the time-dependent problem, employs the method of characteristics, and extends the time integration to infinity such that the steady state is reached [9,10].

A demanding issue remains the better characterization of the general shear-rate dependence of the excess stresses. From the experimental point of view, it should be clarified whether self-assembly shows an extended range of power-law behavior for the viscosity as known from common non-Newtonian liquids. Based on numerical investigation and asymptotic scaling analysis, we have seen that our model does not have this feature, and it remains an open question as to how such a behavior could eventually be built in.

There are a striking number of similarities between the treatment of self-assembly, block copolymer melts, and critical colloidal dispersions under shear. But with respect to self-assembly, there is one crucial complication: the presence of two correlation lengths in the theory. Here we could not express our results in terms of only one dimensionless group that involves the shear rate and the correlation lengths. In the scaling forms, varying combinations of the correlation lengths appear. Furthermore, these are the correlation lengths which are strictly defined only under equilibrium conditions. Obviously, for strong shear, new modified length scales will appear, which will also be direction dependent due to the anisotropic nature of the flow field. A more complete theory should make reference to these inherent scales.

Another interesting point that has not been touched here is the transient kinetic behavior. This concerns both the buildup of the excess stresses when the shear has been switched on and the relaxation to the equilibrium state after the shearing has been stopped. Results in this direction are of appreciable importance, since in practice the fluids are rarely exposed to such ideal steady-state conditions as can only be realized in carefully set up laboratory experiments.

To obtain a better understanding of the phenomena considered in the present paper, it would be helpful to conduct a series of experiments that record the structure factor under shear and the mechanical stress response simultaneously. The experimental verification of the results presented above can be split into two parts. It must first be checked if, at least for low shear rates, the structure factor undergoes the deformations calculated above. In our opinion, this is essentially a geometrical issue, since the modification of the structure factor must reflect the kinematics of the applied flow field. We therefore have some confidence in the results present in this paper. Secondly, the relations between stresses or rheological coefficients and the observed asymmetry of the structure factor have to be established, a more complex issue.

On the more theoretical side, one could think about a renormalization-group treatment to get rid of the cutoff in wave number space introduced above. Moreover, the influence of hydrodynamic fluctuations and the effect of introduc-

ing a separate field for the surfactant have still to be investigated. It must for example be clarified if hydrodynamic fluctuations have a stabilizing or a destabilizing effect on the shear induced structures. Of more concern are the possible implications of hydrodynamic coupling between the aggregates.

Up to now, we also have confined ourselves to the case of a bicontinuous microemulsion, where the Hamiltonian is invariant under sign reversal of the order parameter. It would be interesting to derive the consequences if this symmetry is broken, as in the oil-rich and water-rich regimes. We know from preliminary experimental evidence that there are novel features there. Furthermore, up to now only the structured but disordered region of the phase diagram has been considered. Further work should also be concerned with the three-phase region, where effects due to shear compete with spinodal decomposition, and with the lamellar region.

In summation, then, we have made moderate progress in

studying a simple model of bicontinuous microemulsion. We have outlined the directions in that the model might be progressed. Also, we comment that the most anomalous rheological behavior in microemulsion comes near the percolation transitions, a matter to which we will turn in future works. The issues we discuss here, that is the connection between microstructure and rheology, are at the foundations of many important technological fields from the food industry to paints and oil recovery. It will be important to pursue many of the ideas in depth.

ACKNOWLEDGMENTS

One of the authors (G.P.) is supported by EEC Grant No. R0232 (08823). The authors acknowledge the support of the Digital Equipment Corporation in the development of computational resources.

-
- [1] B. Widom, *J. Chem. Phys.* **84**, 6943 (1986).
 [2] G. Pätzold and K. Dawson, *J. Chem. Phys.* **104**, 5932 (1996).
 [3] C. J. Mundy, Y. Levin, and K. A. Dawson, *J. Chem. Phys.* **97**, 7695 (1992).
 [4] Y. Levin, C. J. Mundy, and K. A. Dawson, *Physica A* **196**, 173 (1993).
 [5] A. Coniglio, P. Ruggiero, and M. Zannetti, *Phys. Rev. E* **50**, 1046 (1994).
 [6] U. M. B. Marconi and F. Corberi, *Europhys. Lett.* **30**, 349 (1995).
 [7] P. Tartaglia (unpublished); J. Rouche (unpublished); A. Maritan (unpublished); B. Gonnella (unpublished).
 [8] A. Onuki, *Phys. Rev. A* **35**, 5149 (1987).
 [9] G. H. Fredrickson, *J. Chem. Phys.* **85**, 5306 (1986); G. H. Fredrickson and R. G. Larson, *J. Chem. Phys.* **86**, 1553 (1987).
 [10] A. Onuki, *J. Chem. Phys.* **87**, 3692 (1987).
 [11] G. H. Fredrickson and E. Helfand, *J. Chem. Phys.* **87**, 697 (1987); **89**, 5890 (1988).
 [12] J. K. G. Dhont and Henk Verduin, *J. Chem. Phys.* **101**, 6193 (1994); Henk Verduin and J. K. G. Dhont, *Phys. Rev. E* **52**, 1811 (1995).
 [13] M. Teubner and R. Strey, *J. Chem. Phys.* **87**, 3195 (1987).
 [14] B. Widom, K. A. Dawson, and M. D. Lipkin, *Physica A* **140**, 26 (1986); K. A. Dawson, *Phys. Rev. A* **35**, 1766 (1987); K. A. Dawson, M. D. Lipkin, and B. Widom, *J. Chem. Phys.* **88**, 5149 (1988); J. R. Gunn and K. A. Dawson, *ibid.* **91**, 6393 (1989); A. Berera and K. A. Dawson, *Phys. Rev. A* **41**, 626 (1990); K. A. Dawson, B. Walker, and A. Berera, *Physica A* **165**, 320 (1990); K. A. Dawson, in *Structure and Dynamics of Strongly Interacting Colloids and Supramolecular Aggregates in Solution*, edited by S.-H. Chen *et al.* (Kluwer, Dordrecht, 1992).
 [15] G. Gompper and M. Schick, *Phys. Rev. Lett.* **65**, 1116 (1990); G. Gompper and S. Zschocke, *Phys. Rev. A* **46**, 4836 (1992); G. Gompper and M. Kraus, *Phys. Rev. E* **47**, 4289 (1993); **47**, 4301 (1993); G. Gompper and M. Schick, in *Phase Transitions and Critical Phenomena*, edited by C. Domb and J. Lebowitz (Academic, London, 1994), Vol. 16.
 [16] P. C. Hohenberg and B. I. Halperin, *Rev. Mod. Phys.* **49**, 435 (1977).
 [17] R. I. Tanner, *Engineering Rheology* (Clarendon, Oxford, 1988).
 [18] Y. Levin, C. J. Mundy, and K. A. Dawson, *Phys. Rev. A* **45**, 7309 (1992).
 [19] C. M. Bender and S. A. Orszag, *Advanced Mathematical Methods for Scientists and Engineers* (McGraw-Hill, Singapore, 1978).
 [20] E. W. Kaler, K. E. Bennett, H. T. Davis, and L. E. Scriven, *J. Chem. Phys.* **79**, 5673 (1983); M. Kolarchyk, S.-H. Chen, J. S. Huang, and M. W. Kim, *Phys. Rev. A* **29**, 2054 (1984); *Phys. Rev. Lett.* **53**, 941 (1984); S.-H. Chen, S.-L. Chang, and R. Strey, *J. Chem. Phys.* **93**, 1907 (1990).
 [21] H. A. Barnes, J. F. Hutton, and K. Walters, *An Introduction to Rheology* (Elsevier, Amsterdam, 1989).
 [22] G. G. Batrouni *et al.*, *Phys. Rev. D* **32**, 2736 (1985); P. Balbuena and K. A. Dawson, *Phys. Rev. B* **38**, 11 432 (1988).